

Properties of hierarchy zeolite obtained from obsidian and perlite

Citation

KURMACH, Mykhailo M., Kateryna M. KONYSHEVA, Kateryna FILATOVA, Svitlana O. SOTNIK, Konstantin S. GAVRILENKO, O.V. ANDREEV, and Oleksij Vasylyovich SHVETS. Properties of hierarchy zeolite obtained from obsidian and perlite. *Theoretical and Experimental Chemistry* [online]. vol. 57, iss. 6, Springer, 2022, p. 451 - 457 [cit. 2023-02-06]. ISSN 0040-5760. Available at <https://link.springer.com/article/10.1007/s11237-022-09715-8>

DOI

<https://doi.org/10.1007/s11237-022-09715-8>

Permanent link

<https://publikace.k.utb.cz/handle/10563/1010912>

This document is the Accepted Manuscript version of the article that can be shared via institutional repository.

PROPERTIES OF HIERARCHY ZEOLITE OBTAINED FROM OBSIDIAN AND PERLITE

M. M. Kurmach,¹ K. M. Konysheva,¹ K. O. Filatova,² S. O. Sotnik,¹ K. S. Gavrilenko,^{3,4} O. V. Andreev,⁵ and O. V. Shvets¹

¹L. V. Pisarzhevsky Institute of Physical Chemistry, NAS of Ukraine, Kyiv, Ukraine. E-mail: alexshvets@ukr.net.

²Tomas Bata University in Zlin, Zlin, Czech Republic.

³LLC Research and Production Enterprise "Enamine", Kyiv, Ukraine.

⁴Research and Production Chemical and Biological Center of Taras Shevchenko National University of Kyiv, Kyiv, Ukraine.

⁵Taras Shevchenko National University of Kyiv, Kyiv, Ukraine.

A method for obtaining hierarchical BEA, MOR, MFI, MTW, and GIS zeolites and nanocomposites by partial recrystallization of perlite and obsidian in the presence of polyquaternary ammonium salts, which act as structure-directing agents, is proposed. The obtained materials are characterized by a developed specific surface, the presence of Lewis (up to 98 $\mu\text{mol/g}$) and Bronsted (5-105 $\mu\text{mol/g}$) acid sites and show catalytic activity in the process of 1,1-diethoxyethane production from acetaldehyde and ethanol.

Keywords: hierarchical zeolite, Gemini surfactant, acetaldehyde, 1,1-diethoxyethane.

Hierarchical zeolite materials are a new class of acid-base catalysts characterized by a developed outer surface and, as a consequence, a high concentration of active sites available for molecules larger than 1 nm [1,2]. Therefore, such materials can be used in various processes of fine organic synthesis, providing a high degree of conversion of bulk substrates, as well as in high-temperature processes, providing a low degree of deactivation of active sites [2, 3]. Several approaches are used to create such catalysts, among which a method using polyquaternary ammonium salts (Gemini type surfactants) as structure-directing agents is the most promising [3]. The peculiarity of such molecules is the simultaneous presence of hydrophilic sites in their structure that perform a structure-directing function, and hydrophobic tails that limit the growth of a crystal in one or more directions [1,4]. This approach promotes the production of hierarchical zeolites consisting of 2 nm thick ultrathin layers (the size of a unit cell for MFI zeolite in the direction of the crystallographic axis b) [2]. Such catalysts show high efficiency in several high-temperature processes, for example in the processes of conversion of methanol into olefins [3], dehydration of various substrates [5], etc. At the same time, their high catalytic activity is combined with the high cost of their production, which significantly complicates their use as catalysts for large-scale processes. The production of hierarchical zeolites using cheap raw materials is one of the ways of reducing the cost of such materials. Expanded perlite and obsidian, which are non-porous natural aluminosilicates with a chemical composition close to zeolite, are considered to be promising "matrices" for the creation of such composite catalysts.

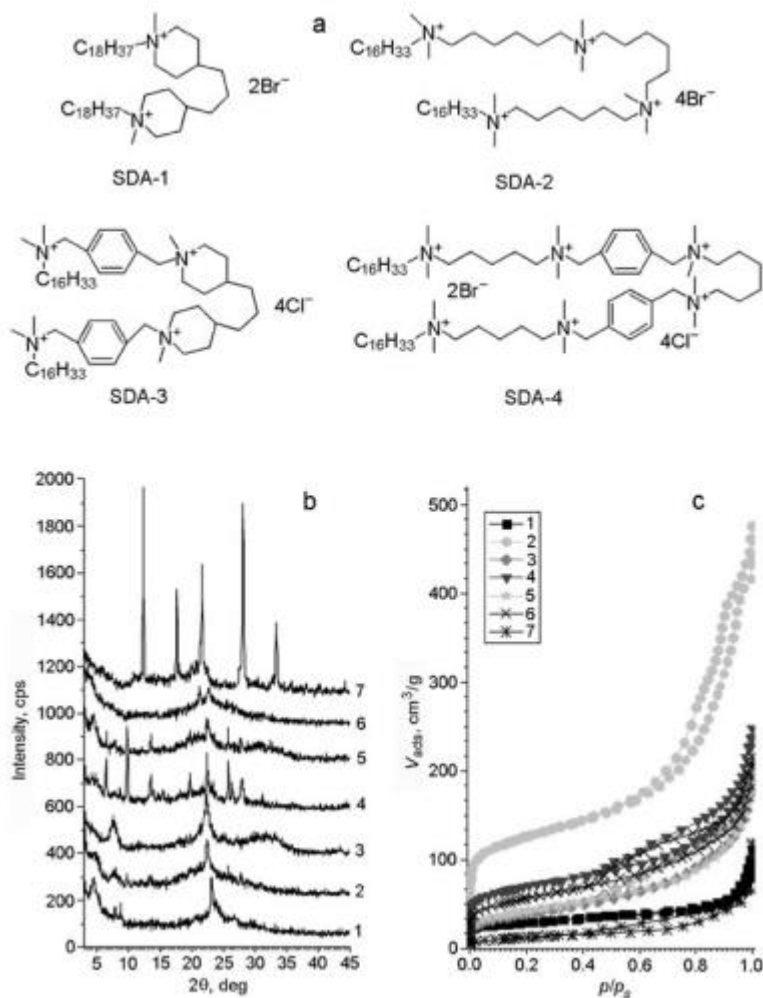


Fig. 1. SDA used for the synthesis of composites (a), diffraction patterns (b), and low-temperature adsorption isotherms (c) of composites based on hierarchical zeolites of different structural types with expanded obsidian and perlite: 1) H_MFI; 2) H-BEA_np; 3) H-BEA_nsh; 4) H-MOR_nsh_per; 5) H-MOR_nsh_obs; 6) H-MTW_nr; 7) H-GIS.

Obsidian and perlite-based materials are widely used as additives to portland cement [6], thermal insulation materials [7], and filter membranes for rapeseed oil purification [8]. Therefore, the use of spent perlite and obsidian as carriers for hierarchical zeolites can significantly reduce the production cost of the latter.

Currently, several zeolite synthesis methods that are using various natural silicates as silicon sources have been developed, which contributes to the production of zeolite materials by their complete recrystallization. For example, the work [9] shows a method of recrystallization of obsidian into Na-A and Na-X. Two-phase systems (nanocomposites) can be formed under incomplete crystallization of expanded perlite or obsidian, in which zeolites will act as an active phase, and the undissolved matrix of perlite or obsidian will act as a carrier.

Therefore, this work aims at studying the effect of template structure and carrier type on the structure (type of formed zeolite phase) of the obtained composites, their structural and sorption, acid and catalytic properties in the process of 1,1-diethoxyethane production from acetaldehyde and ethyl alcohol.

The synthesis of structure-directing agents (Fig. 1a) was performed according to the method described in the works [10, 11]. Expanded perlite or obsidian was used without additional treatment. Acid treatment of the original obsidian or perlite with hydrochloric or nitric acid solutions was performed to obtain a series of zeolite samples, aimed at partial removal of aluminum and alkaline earth elements from aluminosilicate. The removal of aluminum from perlite or obsidian was performed according to the following method: 3 g of perlite or obsidian were mixed with 40 mL of acid solution (1 M), then the mixture was heated to 75°C and kept for 4 h with vigorous stirring; obsidian or perlite powder was filtered, washed with hydrochloric acid, and dried at room temperature overnight. The synthesis of MFI, MOR, BEA, GIS, and MTW zeolites was performed by the following method: the calculated amount of sodium hydroxide and organic structure-directing agent (SDA) was dissolved in water; a source of silicon, such as tetraethyl orthosilicate (TEOS) and aluminum isopropoxide (only for H-BEA_np) was added to the reaction mixture (RM). Ethyl alcohol and then expanded perlite or obsidian were added to the RM after TEOS hydrolysis. Obsidian and perlite were added in a mass ratio of SiO₂:obsidian = 1:0.7. The composition of the reaction mixture for the synthesis of hierarchical MOR zeolites (excluding perlite) is 24 SiO₂:5.9 Na₂O:1.8 SDA:1706 H₂O:192 ethanol. The RM was stirred at 65°C overnight, followed by hydrothermal treatment for 4-13 days in steel autoclaves with stirring. The resulting powder was filtered, washed with distilled water, ethyl alcohol, and dried. The zeolite samples were calcined at 600°C for 5 h (heating rate 5°C/min) to remove the template. The powder, 0.5 g was treated with 30 mL of 1 M NH₄Cl at a temperature of 40°C (16-17 h) to obtain H-forms of these zeolites. The powder was filtered, washed with distilled water, and dried. The procedure was repeated one more time, however, the zeolite was calcined at 450°C.

The phase composition of the synthesized zeolite materials was determined by a Bruker D8 Advance X-ray diffractometer with CuK α radiation ($\lambda = 1.54184$ nm) in the angles range of $2\theta = 3^\circ$ - 45° at intervals of $2\theta = 0.03^\circ$, and a signal accumulation of 3 s/deg. The adsorption properties of the obtained zeolites were studied by low-temperature nitrogen adsorption (-196°C) using a Soptomatic 1990 porous material analyzer. The micropore size distribution was determined by the Saito-Foley method. The values of the external surface of the obtained hierarchical samples were calculated using t-plot and aS methods [12]; the specific surface area was calculated according to the Brunauer-Emmett-Teller equation (BET) [13], while the mesopore size distribution was calculated according to the Barrett-Joyner-Halenda equation (BJH) [14]. The study of the morphology of the obtained samples was performed by a Nova NanoSem 450 scanning electron microscope. The acidic properties of the obtained samples were studied by stepwise pyridine adsorption and desorption with IR spectroscopy control. The samples were pressed into binder-free tablets and activated at 450°C in a vacuum. The samples were saturated by pyridine vapor at 150°C, then the physically sorbed pyridine was removed in a vacuum at the same temperature and samples cooled to room temperature. The IR spectra were recorded by a Perkin Elmer Spectrum One Fourier spectrometer. The desorption of pyridine was performed at temperatures of 150°C, 250°C, 350°C, and 450°C. The concentration of acid sites was determined by the amount of pyridine retained at these temperatures, using the formula given in the work [15]. The catalytic activity of the obtained composites was studied in the process of 1,1-diethoxyethane production from acetaldehyde and ethanol. The experiment was performed according to the following method: 0.05 g of catalyst that was activated at a temperature of 450°C was added to a solution containing 0.05 mol of dodecane (internal standard). Acetaldehyde (0.1 mol) and ethanol (0.2 mol) were added to the reaction mixture, then the reactor was sealed and the reaction mixture

was stirred for 4 h at room temperature. An aliquot was taken, the catalyst was separated by centrifugation, and the sample was analyzed by a gas chromatograph. The yield of 1,1-diethoxyethane was evaluated using the ratio of the peaks of the internal standard and 1,1-diethoxyethane.

The designation of samples: H_MFI is a composite based on expanded perlite and hierarchical MFI zeolite, obtained using SDA-2 (Fig. 1a); H-BEA_np is a composite based on obsidian and hierarchical BEA zeolite structural, obtained using SDA-3; H-BEA_nsh is a composite based on expanded perlite, pre-treated with 1 M of hydrochloric acid solution and hierarchical BEA zeolite, obtained using SDA-1; H-MOR_nsh_per is a composite based on expanded perlite and hierarchical MOR zeolite, obtained using SDA-1; H-MOR_nsh_obs is a composite based on expanded obsidian and hierarchical MOR zeolite, obtained using SDA-1; H-MTW_nr is a composite based on expanded perlite and hierarchical MTW zeolite, obtained using SDA-4; H-GIS is a composite based on expanded perlite and hierarchical MTW zeolite, obtained using SDA-2.

The use of different synthesis conditions allows one to obtain several zeolite structures: BEA, MOR, MFI, MTW, and GIS. The formation of GIS zeolites is observed during recrystallization of perlite or obsidian in the absence of additional sources of silicon or aluminum, due to the high content of aluminum in the initial matrices ($\text{Si/Al} = 7.5$ for perlite and $\text{Si/Al} = 5$ for obsidian) regardless of the type of structure-directing agent. The formation of zeolites of several structural types occurs when SDA-1 is used with two quaternary nitrogen atoms as a template: BEA and MOR, which is typical for the synthesis of “pure” zeolite samples.

TABLE 1. Structural and Sorption Properties of Obsidian and Perlite-Based Composites of Hierarchical Zeolites

Sample	Aluminosilicate	S_{BET} , $\text{m}^2\cdot\text{g}^{-1}$	S_{external} , $\text{m}^2\cdot\text{g}^{-1}$	V_{Σ} , $\text{cm}^3\cdot\text{g}^{-1}$	V_{mezo} , $\text{cm}^3\cdot\text{g}^{-1}$	V_{micro} , $\text{cm}^3\cdot\text{g}^{-1}$
H_MFI	Obsidian	105	50	0.13	0.11	0.02
H-BEA_np	Obsidian	415	215	0.72	0.62	0.10
H-BEA_nsh	Perlite (1 M HCl)	140	130	0.32	0.31	0.01
H-MOR_nsh_per	Perlite	250	125	0.38	0.32	0.06
H-MOR_nsh_obs	Obsidian	150	110	0.31	0.29	0.02
H-MTW_nr	Perlite	200	140	0.32	0.30	0.02
H-GIS	Perlite	45	31	0.15	0.14	0.01

The formation of BEA zeolites (for samples obtained with the low conversion of obsidian and perlite) is initially observed, when TEOS is used as an additional source of silicon and perlite or obsidian that underwent acid treatment; which is probably due to the presence of areas depleted of aluminum on the surface. The degree of recrystallization of perlite or obsidian into zeolite increases when synthesis time is increased; at the same time, the formation of a mixture of phases consisting of BEA and MOR zeolites is observed. The formation of the last zeolite is caused by an increase in the aluminum content in the “volume” of perlite or obsidian. SDA-2 is characterized by the formation of aluminosilicate MFI zeolites at the initial stage of recrystallization, while MTW is formed for SDA-4.

This work studied several composites of hierarchical zeolites of different structural types, such as BEA, MOR, MFI, MTW, and GIS. The original perlite and obsidian are amorphous aluminosilicate materials; thus their diffraction patterns do not contain reflections, while the presence of peaks indicates the formation of other crystalline silica phases. Figure 1b shows diffraction patterns of the samples of zeolite composites of different structural types obtained by recrystallization of perlite and obsidian under different conditions. Reflections are corresponding to the formation of certain zeolite phases for all the studied samples: reflections at $2\theta = 7.5^\circ$ and 22.5° for BEA zeolite; at $2\theta = 7.9^\circ$; 8.8° . and 23.0° for MFI zeolite; at $2\theta = 6.5^\circ$, 9.8° ; 13.6° , 19.7° , 22.4° ; 25.8° for MOR zeolite; signals at $2\theta = 7.5^\circ$, 21.1° , and 22.8° for MTW zeolite; the presence of signals at $2\theta = 12.4^\circ$, 17.7° , 21.7° , 28.1° , and 33.5° for GIS. The intensity of reflections is much lower on diffraction patterns when compared to both “traditional” analogues (which may indicate the formation of small size zeolite particles) and “hierarchical” zeolites, indicating the presence of an additional amorphous phase; particularly perlite or obsidian recrystallization of which does not occur completely.

Figure 1c shows isotherms of low-temperature nitrogen adsorption of the studied samples, while Table 1 shows structural and sorption characteristics of the synthesized composites. All isotherms can be attributed to type IV, which is characteristic of the samples with combined micro- and mesoporosity. The characteristics of the specific surface area and pore volume vary considerably depending on the zeolite structure and the degree of recrystallization of perlite or obsidian. The values of the specific surface area (Table 1) are 45-450 m²/g, and the total pore volume is 0.13-0.72 cm³/g. It should be noted that H-GIS composites with obsidian are characterized by small values of specific surface area (Table 1) and micropore volume; although H-GIS has a higher degree of crystallinity when compared to other composites studied in this work. This may be caused by the small pore size of the zeolite and the unavailability of most of the zeolite phase surface for nitrogen. Low surface values are due to the low content of the zeolite phase in the case of the H_MFI composite, which is confirmed by X-ray phase analysis.

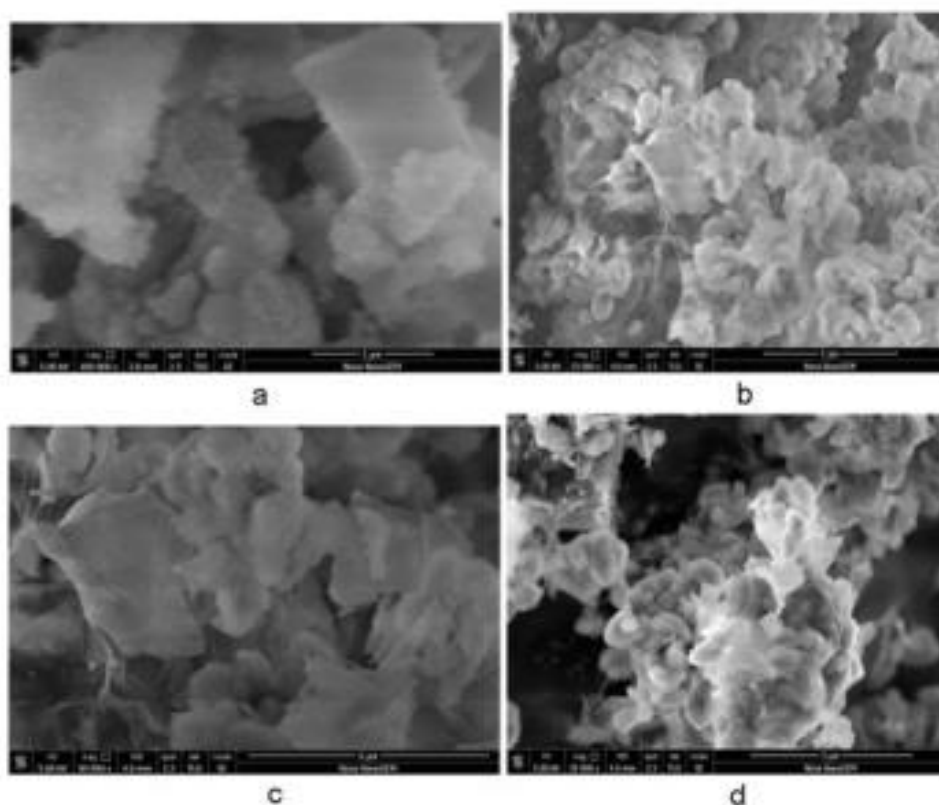


Fig. 2. SEM images of H-BEA_{np} (a, b) and H-MOR_{nsh_per} (c, d) composites.

The H-BEA_np composite obtained using SDA-3 is characterized by the largest specific surface area, which is probably due to the relatively high content of the zeolite phase in the sample. H-BEA_nsh obtained using SDA-1, is characterized by a significantly lower surface when compared to H-BEA_np, due to the lower content of the zeolite phase and the characteristics of BEA zeolites obtained using SDA-1. BEA zeolites obtained using this template are characterized by the formation of layered nanocrystals, as noted in [16, 17]. These materials have low values of the volume of micropores when compared to microporous analogues and nanosponges. It should be noted that the composite obtained using perlite as a carrier has higher values of specific surface area and pore volume when comparing the specific surface area of H-MOR_nsh_per and H-MOR_nsh_obs composites; due to the slightly different nature of the carrier and probably different zeolite phase content in the samples, which also confirms the lower degree of crystallinity of the H-MOR_nsh_obs composite when compared to H-MOR_nsh_per.

Figure 2 shows SEM images of the obtained H-BEA_np and H-MOR_nsh_per composites. According to the images, the main phase is round particles larger than 5 μm in both cases, which can be attributed to perlite or obsidian. In addition to the bulk phase, there are 1 μm particles for H-BEA_np, which can be attributed to the zeolite phase (spongy materials), and the formation of layered elongated crystals chaotically located on the surface of the silica matrix for H-MOR_nsh_per. According to the “pure” synthesis (in the absence of obsidian and perlite in the RM), the formation of sponges is observed for H-BEA_np, which consist of 15 nm nanoparticles; which is indirectly confirmed by the low-temperature nitrogen adsorption data. Similarly, the formation of MOR zeolites with layered nanocrystal morphology is observed in the case of H-MOR_nsh_per.

The concentration of the Lewis and Bronsted acid sites, determined by the stepwise pyridine adsorption and desorption are given in Table 2. All zeolites are characterized by a small concentration of Lewis and Bronsted acid sites: much smaller compared to hierarchical and traditional zeolites with a similar chemical composition. The concentration of the Lewis and Bronsted acid sites is 13 and 12 $\mu\text{mol/g}$ for the H_MFI composite, which correlates with a low value of the specific surface area of the composite and a low proportion of the zeolite phase in the composite. A similar situation is observed in the case of H-BEA_nsh (20 and 15 $\mu\text{mol/g}$). The concentration of the Lewis and Bronsted acid sites is 1 and 5 $\mu\text{mol/g}$ for H-GIS. Such a low concentration of sites is apparently due to the unavailability of sites in zeolite micropores for pyridine molecules. The highest concentration of active sites is typical for the H-BEA_np sample, which is characterized by a high content of the zeolite phase and a high external surface. H-MOR_nsh_obs and H-MOR_nsh_per composites are characterized by the comparable concentration values of Bronsted acid sites. At the same time, the concentration of Lewis acid sites for the sample obtained using perlite is significantly lower when compared to H-MOR_nsh_obs; which can be explained by the different content of the zeolite phase in the samples.

TABLE 2. Acidic Characteristics and Catalytic Activity of Obsidian and Perlite-Based Hierarchical Zeolite

Sample	Concentration of acid sites, calculated after desorption of pyridine at different temperatures, °C								Yield of 1,1-diethoxyethan, %
	Lewis acid sites, $\mu\text{mol/g}$				Bronsted acid sites, $\mu\text{mol/g}$				
	150	250	350	450	150	250	350	450	
H_MFI	13	12	5	0	19	6	0	0	0.37
H-BEA_np	98	104	102	91	105	68	44	0	26.10
H-BEA_nsh	20	16	13	0	15	5	0	0	0.18
H-MOR_nsh_per	45	34	33	12	36	28	16	10	18.37
H-MOR_nsh_obs	18	18	13	6	32	32	11	0	2
H-MTW_nr	34	19	11	0	22	15	12	0	7.59
H-GIS	1	0	0	0	5	0	0	0	0

The catalytic activity of the composites was studied in the process of 1,1-diethoxyethane production from acetaldehyde and ethanol. 1,1-Diethoxyethane is an important additive in motor oils that increases their octane number [18]. The catalytic activity of the synthesized samples differs a lot (Table 2) and significantly depends on the content of the zeolite phase. H_MFI is practically not active in this process, due to the low concentration of active sites in the samples. In the case of H-GIS, both the low concentration and the activity of the catalyst may be because most sites of such zeolite are not available for pyridine molecules and substrate molecules. The highest yield of 1,1-diethoxyethane was achieved for the H-BEA_np and H-MOR_nsh_per samples (26.10 and 18.37%, respectively). Both samples are characterized by the highest concentration of acid sites. At the same time, it should be noted that there is no direct correlation between the activity and concentration of Bronsted acid sites. For example, H-MOR_nsh_obs and H-MOR_nsh_per are characterized by a proportional concentration of Bronsted acid sites, while the second composite is significantly more active in the study process. However, the total concentration of Bronsted and Lewis acid sites in the case of H-MOR_nsh_per significantly exceeds the values obtained for H-MOR_nsh_obs.

Therefore, the method for obtaining hierarchical zeolite composites of different structural types using perlite and obsidian has been developed. It is shown that the structure of the template and the nature of the starting material (expanded perlite or obsidian) determine the zeolite phase content and, as a consequence, the adsorption, acid, and catalytic properties of the obtained composites in the synthesis of 1,1-diethoxyethane from ethanol and acetaldehyde.

REFERENCES

1. W. Schwieger, A. G. Machoke, T. Weissenberger, et al., *Chem. Soc. Rev.*, 45, No. 12, 3353-3376 (2016).
2. M. Choi, K. Na, J. Kim, et al., *Nature*, 461, 246-249 (2009).
3. J. Kim, M. Choi, and R. Ryoo, *J. Catal.*, 269, No. 1, 219-228 (2010).
4. Y. Zhang, X. Shen, Z. Gong, et al., *Chem. Eur. J.*, 25, No. 3, 738-742 (2019).
5. J. Shan, Z. Li, S. Zhu, et al., *Catalysts*, 9, No. 2, 121-136 (2019).
6. W. A. Cordon, *Lightweight Concrete Products and a Process of Producing Same*, Patent US 3565650, Publ. 1971.
7. Y. Takeuchi, *High Temperature Insulating Structure*, Patent US 3991254, Publ. 1976.
8. S. K. Palm, T. R. Smith, J. C. Shiu, and J. S. Roulston, *Filterable Composite Adsorbents*, Patent US 6712974, Publ. 2004.
9. C. A. Rios, C. D. Williams, and O. M. Castellanos, *Ing. Compet.*, 14, No. 2, 125-137 (2012).
10. M. M. Kurmach, P. S. Yaremov, V. V. Tsyryna, et al., *Theor. Exp. Chem*, 51, No. 4, 216-223 (2015).
11. K. Cho, K. Na, J. Kim, et al., *Chem. Mater*, 24, No. 14, 2733-2738 (2012).
12. B. C. Lippens and J. De Boer, *J. Catal.*, 4, No. 3, 319-323 (1965).
13. S. Brunauer, P. H. Emmett, and E. Teller, *J. Am. Chem. Soc.*, 60, No. 2, 309-319 (1938).
14. E. P. Barrett, L. G. Joyner, and P. P. Halenda, *J. Am. Chem. Soc.*, 73, No. 1, 373-380 (1951).
15. C. Emeis, *J. Catal.*, 141, No. 2, 347-354 (1993).
16. E. M. Konyshva, T. M. Boychuk, and A. V. Shvets, *Theor. Exp. Chem*, 52, No. 2, 90-96 (2016).
17. M. M. Kurmach, N. A. Popovych, P. I. Kyriienko, et al., *Theor. Exp. Chem*, 53, No. 2, 122-129 (2017).
18. M. A. R. Capeletti, L. Balzano, G. de la Puente, et al., *Appl. Catal. A*, 198, Nos. 1-2, L1-L4 (2000).